ARCHIVES OF ELECTRICAL ENGINEERING VOL. 65(4), pp. 843-854 (2016)

DOI 10.1515/aee-2016-0059

# Kriging based robust optimisation algorithm for minimax problems in electromagnetics

YINJIANG LI, MIHAI ROTARU, JAN K. SYKULSKI

*Electronics and Computer Science*
*University of Southampton*
*Southampton, United Kingdom*
*e-mail: jks@soton.ac.uk*

(Received: 19.07.2016, revised: 12.09.2016)

**Abstract:** The paper discusses some of the recent advances in kriging based worst-case design optimisation and proposes a new two-stage approach to solve practical problems. The efficiency of the infill points allocation is improved significantly by adding an extra layer of optimisation enhanced by a validation process.

**Key words**: worst-case optimisation, minimax problems, kriging, robust design

## 1. Introduction

It is often the case that sampling in modern engineering design may be constrained due to considerations of computational costs, time and thus available resources. In the context of electromagnetic design – where nowadays numerical simulation tools need to be used, such as the finite element method (FEM) – repetitive evaluation of the objective function may take hours or days of computation making the design process impractical. When extensive sampling is not available, surrogate based optimisation may significantly improve the design efficiency.

## 2. Worst-case problem specification

Robust optimisation is a relatively new term, its history can be dated back to 1989 when Taguchi first introduced the concept of design quality [1], and since then optimisation involveing uncertainties has been increasingly drawing more attention. Due to the complexity of the optimisation problems in engineering design, the high level of non-linearity means these problems cannot be closely approximated by single linear or quadratic functions. Therefore, these problems are often solved by using direct search global optimisation algorithms. When evaluation of the underlying problem is expensive in terms of time or cost, surrogate modelling techniques are often implemented as an approximation and optimisation is applied to the surrogate model instead of the original problem.

The output *f* of a black-box function, when the input variable *x* contains deterministic type of uncertainties, can be expressed by a simplified equation (ignoring possible other sources of uncertainties and assuming the uncertainty ε is independent of the input variable *x*) [2]

$$f = f(x+\varepsilon), \tag{1}$$

where ε[–ε, ε], the distribution of uncertainty ε, is unknown, but the magnitude is bounded by a given range ε.

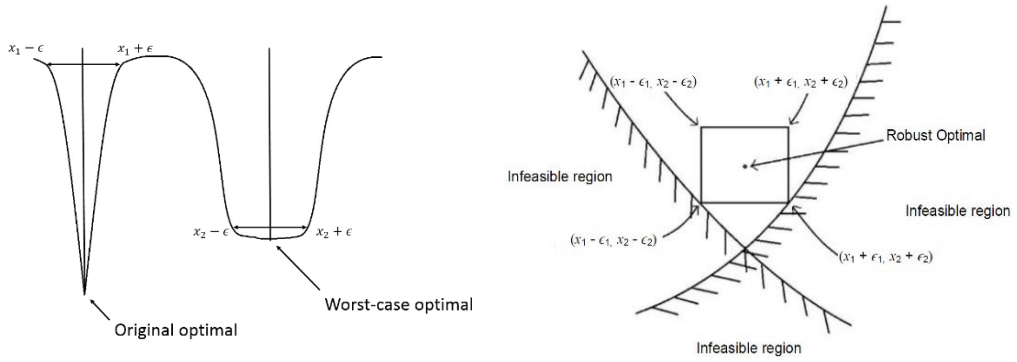


Fig. 1. Worst-case examples. 1 – 1D example, 2 – 2D example with constraints

Two simple examples are given in Fig. 1. The 1D illustration shows that, depending on the size of the uncertainty ε, the preferred worst-case robust optimum may differ from the original (theoretical) optimal point, as when the parameter varies within the specified limits (e.g. imposed by manufacturing tolerances) the performance worsens significantly, whereas the robust optimum ensures good performance throughout. The 2D example illustrates that the worst-case optimum needs to consider design constraints, as the optimum solution with uncertainties must not violate the infeasible region.

## 3. A brief review of existing approaches

For a deterministic type of uncertainties, the basic approach is to transform the robust optimisation problem into a standard optimisation problem by optimising the worst-case of the original objective function, where multiple objective function evaluations are needed at each design stage. The number of objective function calls may be significantly increased and many unimportant and possibly nearly duplicated design points will be allocated during this process and thus making the optimisation extremely inefficient. This large number of function calls will be of particular concern to designers, especially when the objective function is expensive to evaluate, which is often the case in electromechanical or electromagnetic design where the main tool for field modelling involves numerical computation (such as finite elements).

Recently, some more efficient kriging based approaches for solving worst-case optimisation problems have been proposed in literature. The authors of [3] use the mean and variants to

assess the robustness, while their proposed strategy utilises the gradient information computed from the kriging model. In [4] the Expected Improvement (*EI*) infill sampling approach is combined with a relaxation procedure based on a kriging model. In [5] the *EI* infill sampling approach is applied to the worst-case response surface calculated based on the kriging model.

## 4. A two stage approach

In this paper, we propose a two-stage approach for solving computationally expensive worst-case optimisation problems. We focus on maximising the usage of available information while delaying the calculation of the worst-case value at sampling points to achieve a more efficient sampling scheme for the worst-case type of robust design optimisation.

The worst-case optimisation problem is often referred to as the minimax problem, with an extra 'layer' of optimisation, therefore the infill sampling criteria for global optimisation are often found inappropriate in the context of such problems. The worst-case value of the objective function at any given point does not depend on information given by that point alone (including the kriging prediction, mean squared error MSE, gradient etc.), as information from its neighbouring points also needs to be taken into account.

The algorithm consists of two stages: the first one is to update the kriging model by sequentially adding infill points at each iteration based on the worst-case expected improvement (*WCEI*) – this expected improvement measure is recalculated from standard *EI*, by taking the minimal *EI* value within the worst-case region of that design point (design site)

$$WCEI(x) = \max\{\min[EI(x+\varepsilon)],0\}, \tag{2}$$

$$x+\varepsilon \in X,$$

where $X$ is a set of points located within the worst-case region of the unknown point $x$. A 1D example is illustrated in Fig. 2, where the boundary ε of the worst-case design is ±0.3.

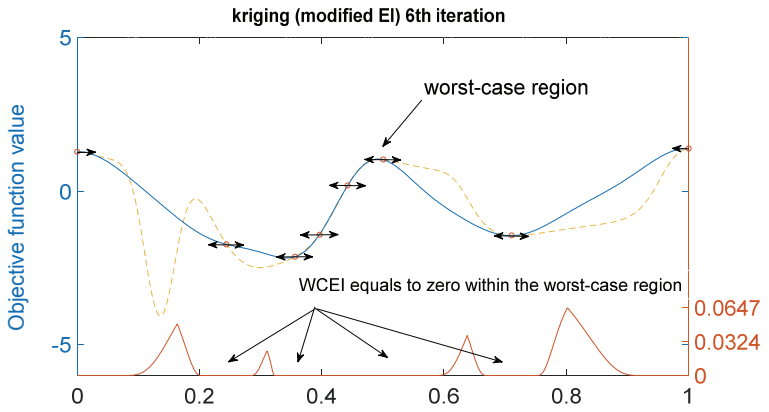


Fig. 2. The worst-case regions of existing design sites in a 1D example

The extra layer of the minimax problem is embedded within the *WCEI*; the new infill sampling point will be located where the minimal expected improvement around the target point is the largest. The *WCEI* is equal to zero at the locations within the worst-case region of existing design sites; consequently, these areas are banned as future infill locations at the model updating stage. During the process of model updating, the worst-case estimation of the objective function is computed simultaneously based on the kriging model constructed using the existing design sites at that iteration.

The second stage is triggered when the maximum *WCEI* within the design space becomes less than a predefined value or stage one has exceeded its allowance, if such limit has been imposed. An exploitation process takes place in stage two; the worst-case region around the worst-case optimum is exploited and validated using a modified *EI* approach, where instead of calculating the improvement, an expected 'deterioration' is estimated to give an indication where the maximal worsening is located within the worst-case region of the worst-case optimum

$$E[D(x)] = \begin{cases} \left(\hat{y}(x) - y_{wc}\right)\Phi\left(u(x)\right) + \hat{s}\phi(u), & s > 0 \\ 0, & s = 0 \end{cases}, \tag{3}$$

$$u = \frac{\hat{y}(x) - y_{\min}}{\hat{s}(x)}.$$

This process is repeated until the value of the expected deterioration is zero or smaller than a predefined value; at this stage the location of the worst-case estimated optimum is added as the next infill point and the associated objective function is evaluated. When the range of the underlying objective function surface is large, both the location and value of the actual worst-case optimum can differ from the estimated one; therefore, the above validation process provides a more accurate prediction within the area of interest, and thus helps the program to locate the best worst-case optimum both efficiently and accurately.

## 5. Example

The worst-case optimisation routine following the two-stage approach is first illustrated using a one-dimensional test example. Fig. 3 shows the original test function and its associated worst-case distribution, where the 'boundary' ε of the worst-case design was assumed to be ±0.3. It can be observed that both the landscape and in particular the position of the optimum differ noticeably between the original function and the worst-case version.

In Fig. 4 (a) to (f) the yellow dotted line depicts the objective function (the worst-case version in (b) and (f), the original shape elsewhere), while the blue bold line shows the kriging prediction. Fig. 4(a) shows the kriging model after the $11^{th}$ iteration. As the maximum *WCEI* within the design space is less than the predefined value of $10^{-3}$, the program enters stage two and the region around the worst-case estimated optimum at $x = 0.12$ (see Fig. 4(b)) is exploited. The infill criterion in Fig. 4(c) illustrates the value of expected deterioration within

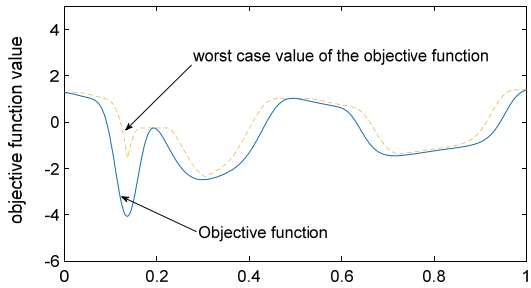


Fig. 3. The original test function and its worst-case value

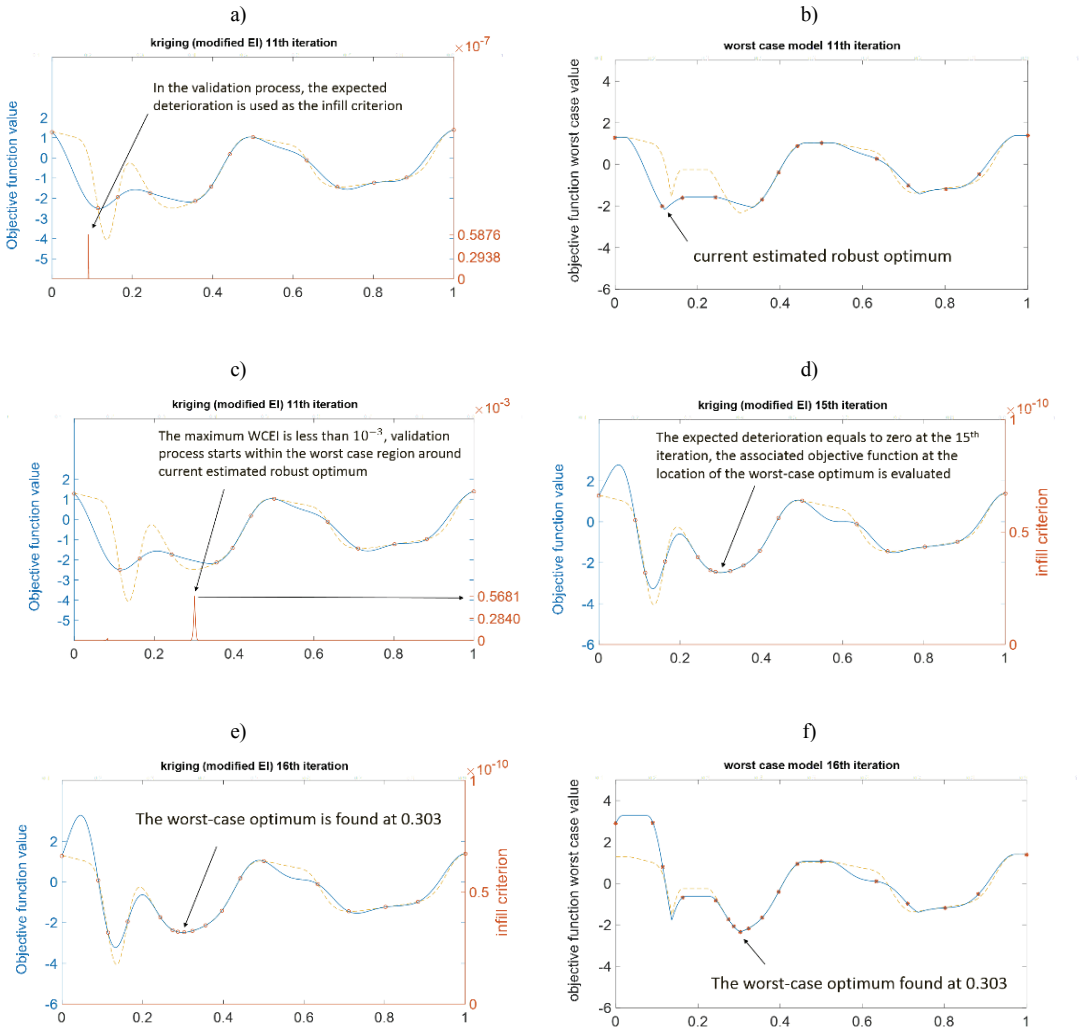


Fig. 4. The proposed algorithm solving a 1D test problem

this region. The estimated worst-case optimum is updated during the validation process and the exploitation area is then moved to a region around the new estimated worst-case optimum at $x = 0.353$. In Fig. 4(d) the value of expected deterioration equals to zero at the 15$^{th}$ iteration; the final worst-case optimum is then located at $x = 0.303$ in Fig. 4(e), while Fig. 4(f) shows the final shape of the estimated worst-case objective function, as well as the actual worst-case objective function.

## 6. Gradient decent with multi-start algorithm for infill points selection

In the context of global optimisation based on surrogate modelling, the location of the next sampling point is based on the infill point sampling scheme which contains a set of rules or formulae. Taking standard Expected Improvement (*EI*) approach as an example, it takes the predicted function value, estimated error and the current optimal value as the input variables, and yields the expected improvement for that particular point; the point with the largest expected improvement will be the next infill point. In order to locate reliably the point with the maximum *EI*, all points within the design space need to be considered, necessitating the calculation of the predicted objective function and the corresponding MSEs at all points. Using an exhaustive method to locate the point with the maximum *EI* is relatively straightforward in a 1D scenario, but may not be acceptable (or practical) in multidimensional cases, where the number of *EI* calculations increases exponentially if the same sampling interval of *EI* is maintained.

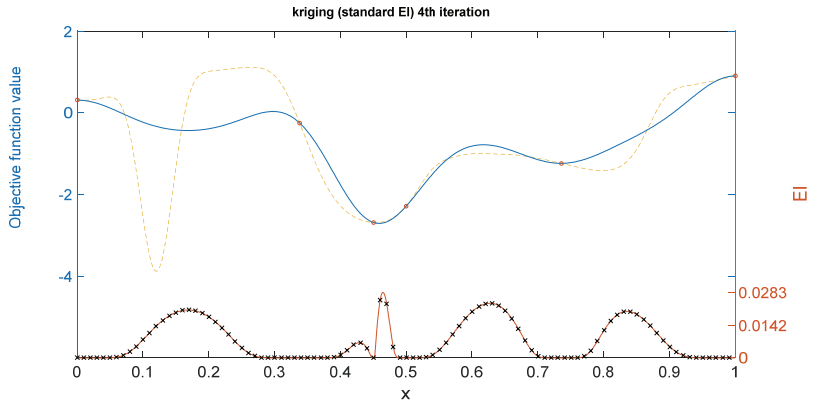


Fig. 5. *EI* at predefined sampling locations for a 1D test function

Figure 5 illustrates a 1D example problem, showing the original objective function (dotted yellow line) and the kriging model (bold blue line), while the bold cinnabar line at the bottom (with crosses on top) is the true *EI* curve. 101 *EI* sampling locations have been evenly distributed within the design region with a fixed interval of 0.01, with the small black crosses on top of the *EI* curve marking the sampled *EI* at those predefined locations. As can be seen from

the figure, the sampled *EI* is a reasonable approximation of the true *EI* curve, but not very accurate at the 'critical' location around the maximum *EI*.

The *EI* curve in Fig. 5 exhibits certain useful characteristics: it is differentiable and the local maximum between two existing design points is often close to their mid-point. We could take advantage of these features in order to significantly speed up the infill sampling process. Instead of using an exhaustive search of all predefined locations, a gradient decent approach with a starting point in the middle between two design points has been incorporated into the algorithm and is illustrated by an example in Fig. 6.

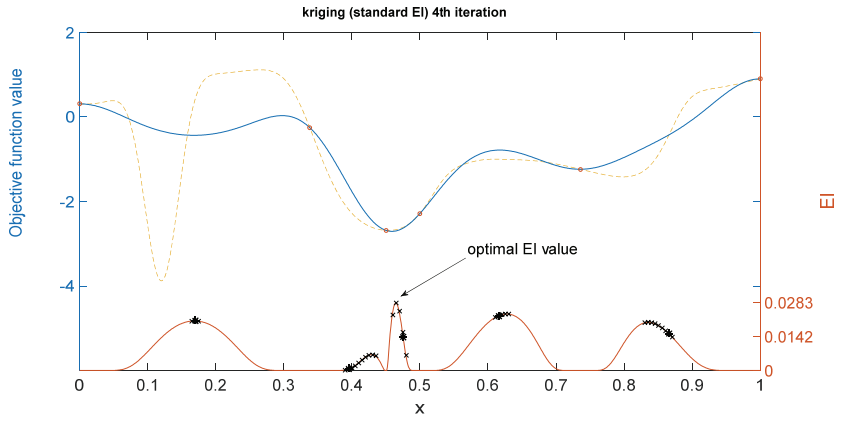


Fig. 6. A gradient decent approach for the *EI* search

In the example given in Fig. 6, the search for the maximum *EI* is not restricted by the pre-defined step size, the optimal *EI* is found with reasonable accuracy while reducing the number of *EI* calculations by half.

For a multidimensional design space, where the local maximum *EI* is located in between multiple existing design sites, a multi-start strategy can be applied to replace a single starting point, as in the 1D case, by simply generating starting points in the middle of each pair of two existing design sites. It is a combination problem and the number of starting points $p$ for $n$ known points is $p = nC2$. Hence for 100 existing design points, 4950 starting points for the gradient decent calculations are generated.

## 7. Solving practical problems

TEAM workshop problems [6] consist of a set of practical electromagnetic optimisation design problems for benchmarking the performance of algorithms. Here we test the proposed approach on two practical benchmark problems. For both problems, the uncertainty boundary for each design parameter (upper and lower limit) is defined as 1% of their given design range.

The superconducting magnetic energy storage device in TEAM problem 22 [7] contains two superconducting coils; the design objective is to achieve a minimal stray field while the

stored energy should be equal to 180 MJ. The configuration of the inner coil is given in the 3 Parameter ('discrete') case, and therefore there are three parameters to be optimised, namely the radius $R_2$, height $h_2$ and thickness $d_2$ of the outer coil, as indicated in Fig. 7.

The objective function is given as

$$OF = \frac{B_{\text{stray}}^2}{B_{\text{norm}}^2} + \frac{|E - E_{\text{ref}}|}{E_{\text{ref}}}, \tag{4}$$

where $E_{\text{ref}} = 180$ MJ, $B_{\text{norm}} = 3$ μT and $B_{\text{stray}}^2$ is defined as

$$B_{\text{stray}}^2 = \frac{\sum_{i=1}^{n=22} |B_{\text{stray},i}|}{22}, \tag{5}$$

subject to the following inequality constraint, known as the quench condition

$$|J| + 6.4|B| - 54.0 \le 0, \tag{6}$$

where $J$ (in $A/mm^2$) is the current density and $B$ the maximum magnetic flux density (Fig. 8).

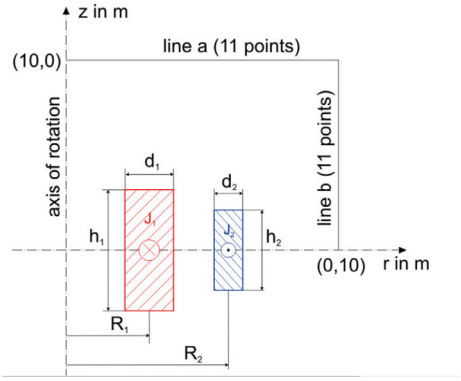


Fig. 7. The superconducting magnetic energy storage device [6, 7]

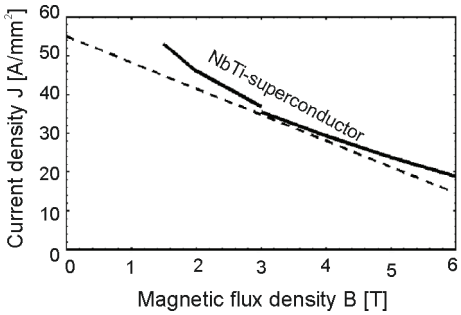


Fig. 8. Critical curve of an industrial superconductor [6, 7]

Table 1. Comparison of performance of various optimisation methods (TEAM 22 problem)

| Algorithm | Optimal value | $R_2$ | $d_2$ | $h_2/2$ | No of function calls |
|---|---|---|---|---|---|
| **GA** | 0.134 | 3.040 | 0.386 | 0.240 | 2400 |
| **SA** | 0.098 | 3.078 | 0.390 | 0.237 | 5025 |
| **HuTS** | 0.089 | 3.080 | 0.380 | 0.246 | 3821 |
| **NTS** | 0.089 | 3.080 | 0.370 | 0.254 | 1800 |
| **PBIL** | 0.101 | 3.110 | 0.421 | 0.241 | 3278 |
| **Kriging *EI*** | 0.0875 | 3.090 | 0.394 | 0.236 | 211 |
| **Kriging *AWEI*** | 0.0875 | 3.090 | 0.400 | 0.232 | 323 |
| **Kriging *WCEI* (worst case)** | 0.1459 | 3.021 | 0.391 | 0.250 | 277 |

Genetic algorithm GA [9]; Stimulated Annealing SA [10]; Tabu Search HuTS [11]; Universal Tabu search [12]; New Tabu Search NTS [13]; Kriging *EI* [14]; Kriging *AWEI* [14]

Table 1 summarises the findings, citing the results from other publications and adding the robust 'worst-case' design. The kriging assisted optimisation has performed consistently well by achieving a marginally better solution with much reduced effort (the number of necessary function calls reduced by almost an order of magnitude). The robust optimum is – perhaps not surprisingly – a little different, slightly worse in terms of the value of the achieved objective function but assuring the robustness within the specified 1% uncertainty of parameters, while preserving the efficiency of computation (small number of function calls).

The device in Problem 25 [6, 8] is a die press with an electromagnet for the orientation of magnetic powder to produce an anisotropic permanent magnet. The objective is to optimise the shape of the model (Fig. 9). The shape g-h of the inner die mold is assumed to be a circle, the inside shape i-j-m of the outer die mold is elliptical and the line j-k is parallel to the *x*-axis; the ampere-turns of the coil are chosen as 4253 A.

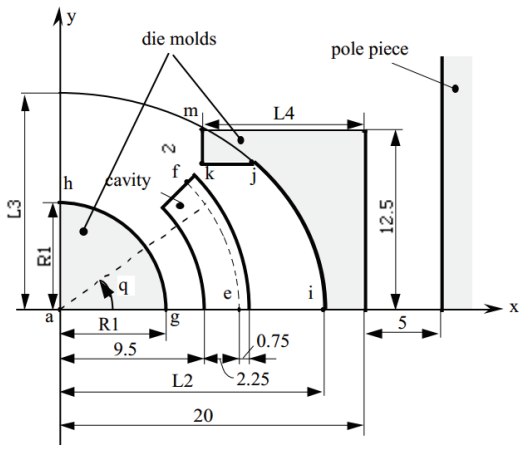


Fig. 9. A model of the die press with an electromagnet [6, 13]

In Fig. 9, R1, L2, L3 and L4 are the design parameters to be optimised so that the objective function $W$ is minimized

$$W = \sum_{i=1}^{n} \left\{ \left( B_{xip} - B_{xio} \right)^2 + \left( B_{yip} - B_{yio} \right)^2 \right\} \tag{7}$$

where $B_x$ and $B_y$ are the $x$ and $y$ components of magnetic flux density at points along the curve e-f, while subscripts $p$ and $o$ denote the calculated and desired values, respectively. The constraints are listed in Table 2 and results in Table 3.

Table 2. Constraints of the parameters

| Variable | Lower-boundary (mm) | Upper-boundary (mm) |
|---|---|---|
| R1 | 5 | 9.4 |
| L2 | 12.6 | 18 |
| L3 | 14 | 45 |
| L4 | 4 | 19 |

Table 3. Comparison of performance of various optimisation methods (TEAM 25 problem)

| Algorithm | Optimal value ($10^{-4}$) | R1 (mm) | L2 (mm) | L3 (mm) | L4 (mm) | No of function calls |
|---|---|---|---|---|---|---|
| **GA** | 2.6861 | 7.2996 | 14.174 | 14.001 | 14.326 | 3421 |
| **SA** | 1.6223 | 7.2252 | 14.322 | 14.110 | 14.306 | 2145 |
| **HuTS** | 0.5009 | 7.3780 | 14.613 | 14.371 | 14.204 | 1580 |
| **UTS** | 1.0501 | 7.5487 | 14.908 | 14.506 | 14.416 | 931 |
| **NTS** | 0.6482 | 7.4337 | 14.732 | 14.428 | 14.237 | 575 |
| **Kriging *EI*** | 0.4527 | 7.2 | 14.1 | 14 | 14.5 | 265 |
| **Kriging *AWEI*** | 0.4125 | 7.2 | 14 | 14 | 14.5 | 214 |
| **Dual kriging** | 0.3231 | 7.1 | 13.9 | 14.014 | 14.273 | 234 |
| **Kriging *WCEI* (worst case)** | 5.4442 | 7.104 | 13.891 | 14.035 | 14.270 | 453 |

Genetic algorithm GA [9]; Stimulated Annealing SA [10]; Tabu Search HuTS [11]; Universal Tabu search [12]; New Tabu Search NTS [13]; Kriging *EI* [14]; Kriging *AWEI* [14]; Dual kriging [15]

The main observations resulting from the TEAM 25 study are broadly in line with what was demonstrated before, although on this occasion the robust optimum is clearly somewhat 'worse' (in absolute terms, but of course it is more robust) and the algorithm is computationally a little less efficient, although still comfortably outperforms other non-kriging methods. It is also interesting to note that for both TEAM problems the originally published results (when the problems were first suggested) appear to be reasonably robust, more so than the subsequently offered solutions. The most important conclusion, however, resulting from this study is that the kriging assisted optimisation is very reliable and offers superbly efficient

computation, both for the 'traditional' (global) optimisation and the robust formulation. Finally, the worst case (minimax) approach appears to be a very helpful methodology for robust optimisation.

## 8. Conclusions

A two-stage approach to worst-case optimisation problems has been proposed and details of the algorithm discussed. The suggested method does not compute the worst-case value, or the corresponding robustness measure, for any design site during the model updating stage, in order to avoid the objective function evaluation at a location that would contribute less to the overall model landscape, which would have taken place if the worst-case value had been evaluated for the newly added infill point. Instead, the explicit search for the robust optimum takes place in the second stage after the model updating process has completed, with a validation process added to exploit the region around the estimated worst-case optimum. A more efficient infill criterion selection algorithm has been introduced. The proposed optimisation method has been validated using simple test functions and two multi-dimensional practical electromagnetic design problems TEAM 22 and TEAM 25. The test results indicate that, with the aid of kriging surrogate modelling techniques, the proposed methodology significantly reduces the number of FEM function calls compared to other methods and thus is computationally very efficient for both global and robust optimisation.

## References

[1] Taguchi G., *Introduction to Quality Engineering*, American Supplier Institute (1989).
[2] Beyer H.G. Sendhoff B., *Robust optimisation – A comprehensive survey*, Comput. Methods Appl. Mech. Engrg., vol.196, pp. 3190-3218 (2007).
[3] Lee K-H., Kang D-H., *A Robust Optimization Using the Statistics Based on Kriging Metamodel*, Journal of Mechanical Science and Technology *(KSME Int. J.),* vol. 20, no. 8, pp. 1169-1182 (2006).
[4] Marzat J., Walter E., Piet-Lahanier H., *Worst-case global optimisation of black-box functions through Kriging and relaxation*, Journal of Global Optimisation*,* Springer Verlag, vol. 55, no. 4, pp. 707-727 (2013).
[5] Rehman S., Langelaar M., van Keulen F., *Efficient Kriging-based robust optimisation of unconstrained problems,* Journal of Computational Science, volume 5, Issue 6, pp. 872-881 (2014).
[6] http://www.compumag.org/jsite/team.html, accessed October (2016).
[7] Alotto P.G., Baumgartner U., Freschi F. et al., *SMES Optimisation Benchmark: TEAM Workshop Problem 22*, Graz, Austria (2008).
[8] Takahashi N., Ebihara K., Yoshida K. et al., *Investigation of simulated annealing method and its application to optimal design of die mold for orientation of magnetic powder*, IEEE Trans. Magn., vol. 32, no. 3, pp. 1210-1213 (1996).
[9] Holland J.H., *Adaptation in Natural and Artificial Systems: An Introductory Analysis with Applications to Biology, Control, and Artificial Intelligence*, Cambridge, MA, USA: MIT Press (1975).
[10 ]Kirkpatrick S., Gelatt C.D., Jr., Vecchi M.P., *Optimisation by simulated annealing*, Science, vol. 220, no. 4598, pp. 671-680 (1983).
[11] Hu N., *Tabu search method with random moves for globally optimal design*, Int. J. Num. Methods Eng., vol. 35, no. 5, pp. 1055-1070 (1992).

[12] Santner T.J., Williams B.J., Notz W.I., *The Design and Analysis of Computer Experiments*, New York, USA, Springer-Verlag (2003).
[13] Hajji O., Brisset S., Brochet P., *A new Tabu search method for optimisation with continuous parameters*, IEEE Trans. Magn., vol. 40, no. 2, pp. 1184-1187, Mar (2004).
[14] Xiao S., Rotaru M., Sykulski J.K., *Six Sigma Quality Approach to Robust Optimisation*, IEEE Trans. Magn., vol. 51, no. 3 (2015).
[15] Li Y., Xiao S., Rotaru M., Sykulski J.K., *A Dual Kriging Approach with Improved Points Selection Algorithm for Memory Efficient Surrogate Optimisation in Electromagnetics*, IEEE Transactions on Magnetics, vol. 52, no. 3, pp. 1-4 (2015).